Journal of Solid Mechanics Vol. 6, No. 1 (2014) pp. 98-121

Investigation of the Effect of Pre-Stressed on Vibration Frequency of Rectangular Nanoplate Based on a Visco-Pasternak Foundation

M. Goodarzi[1,*], M. Mohammadi[1], A. Farajpour[2], M. Khooran[3]

[1]*Department of Mechanical Engineering, College of Engineering, Ahvaz Branch, Islamic Azad University, Ahvaz, Iran*
[2]*Young Researches and Elites Club, North Tehran Branch, Islamic Azad University, Tehran, Iran*
[3]*Department of Mechanical Engineering, Shahid Chamran University of Ahvaz, Ahvaz, Iran*

Received 8 December 2013; accepted 26 January 2014

ABSTRACT

In the present work, the free vibration behavior of rectangular graphene sheet under shear in-plane load is studied. Nonlocal elasticity theory has been implemented to study the vibration analysis of orthotropic single-layered graphene sheets (SLGSs) subjected to shear in-plane load. The SLGSs is embedded on a viscoelastic medium which is simulated as a Visco-Pasternak foundation. Using the principle of virtual work, the governing equations are derived for the rectangular nanoplates. Differential quadrature method (DQM) is employed and numerical solutions for the vibration frequency are obtained. The influence of surrounding elastic medium, material property, aspect ratio, nonlocal parameter, length of nanoplate and effect of boundary conditions on the vibration analysis of orthotropic single-layered graphene sheets (SLGSs) is studied. Six boundary conditions are investigated. Numerical results show that the vibration frequencies of SLGSs are strongly dependent on the small scale coefficient and shear in-plane load. The present analysis results can be used for the design of the next generation of nanodevices that make use of the vibration properties of the graphene.

Keywords: Vibration; Graphene sheet; Shear in-plane load; Visco-Pasternak foundation

1 INTRODUCTION

NANOSTRUCTURES are widely used in micro and nano-scale devices and systems such as biosensors, atomic force microscopes, micro-electro-mechanical systems (MEMS) and nano-electro-mechanical systems (NEMS) due to their superior mechanical, chemical, and electronic properties [1]. Due to the rapid development of technology, especially in micro- and nano-scale fields, one must consider small scale effects and atomic forces to obtain solutions with acceptable accuracy. Neglecting these effects in some cases may result in completely incorrect solutions and hence wrong designs.In such applications, size effects have been experimentally observed [2-4]. As conduction of experiments in nano-level are difficult to control and theoretical atomistic models [5] are computationally intensive for relatively large scale nanostructures, the continuum and semi-continuum [6-8] models have been proven to be important tools in the study of the nanostructures.Classical continuum theories do no account for such size effects due to lack of material length scale parameters. Thus, size-dependent continuum theories such as classical couple stress theory [9,10], modified couple stress theory [11,12], nonlocal elasticity theory [13-17], and strain gradient theory [18-23] have been developed. Among these theories, the nonlocal

* Corresponding author. Tel.: +98 9369712728.
E-mail address: mz.goodarzi.iau@gmail.com (M. Goodarzi).

elasticity theory initiated by Eringen [22, 23] is the most commonly used theory. Unlike classical continuum theories which assume that the stress at a point is a function of strain at that point, the nonlocal elasticity theory assumes that the stress at a point is a function of strains at all points in the continuum. In this way, the size effects could be considered in the constitutive equations simply as a material parameter.

Understanding the vibration behavior of nanostructures is the key step for many NEMS devices. A lot of work has already been done on the continuum models for vibration analysis of carbon nanotubes (CNTs) or similar micro or nanobeam like elements [24-28]. Behfar and Naghdabadi [6] investigated the vibration behavior of multi-layer graphene sheets embedded in an elastic medium. Sakhee-Pouri et al [7] investigated the behaviour of SLGS using molecular structural mechanics. Moosavi et al. [28] investigated vibration analysis of nanorings using nonlocal continuum mechanics and shear deformable ring theory. In their article, they show that the nonlocal effects play an important role in the vibration of nanorings and cannot be neglected. Murmu and Pradhan, [29] applied nonlocal Timoshenko theory and DQM for the stability analysis of embedded single-walled carbon nanotubes. Yi-Ze Wang et al. [30] studied the vibration of double-layered nanoplate. In their research, it is concluded thermal effect and nanoplate with isotropic mechanical properties. It has been reported that graphene sheets have orthotropic properties [31]. Malekzadeh et al. [32] used the DQM to study the thermal buckling of a quadrilateral nanoplates embedded in an elastic medium. Aksencer and Aydogdu [33] proposed levy type solution for vibration and buckling of nanoplate. In that paper, they considered rectangular nanoplate with isotropic property and without effect of elastic medium. Thermal vibration analysis of orthotropic nanoplates based on nonlocal continuum mechanics were studied by Satish et al. [34] who considerate two variable reinfined plate theory for thermal vibration of orthotropic nanoplate. In general, single layered graphene sheets are embedded in an elastic medium but they didn't consider effect of elastic medium in that paper. On the other hand, they represented vibration frequency of rectangular nanoplate only for simply supported boundary conditions and they didn't represent vibration frequency for other boundary conditions. Prasanna Kumar et al. [35] represent thermal vibration analysis of monolayer graphene sheet embedded in an elastic medium via nonlocal continuum theory. In their paper, they consider simply support boundary condition and they don't study other boundary condition. They investigated graphene sheet with isotropic property. Farajpour et al. [36] studied axisymmetric buckling of the circular graphene sheets with the nonlocal continuum plate model. In this paper, the buckling behavior of circular nanoplates under uniform radial compression is studied. Explicit expressions for the buckling loads are obtained for clamped and simply supported boundary conditions. It is shown that nonlocal effects play an important role in the buckling of circular nanoplates. Mohammadi et al. [37] studied the free transverse vibration analysis of circular and annular graphene sheets with various boundary conditions using the nonlocal continuum plate model. They are obtained explicit relations for natural frequencies through direct separation of variables. They applied new version of DQM for vibration analysis of embedded single-layer circular nanoplate. Mohammadi et al. [38] investigated buckling of orthotropic rectangular nanoplate under shear in-plane load. In their paper, the effect of polymer matrix is modeled with Pasternak elastic medium. It is shown that shear in-plane load play important role in buckling analysis of orthotropic rectangular nanoplate.

However, to date, no report has been found in the literature on the influence of shear in-plane loads on the vibration of the SLGSs. Motivated by this idea, we aim to study the nonlocal vibration response of the SLGSs resting on a Visco-Pasternak foundation. The influence of the surrounding elastic medium on the vibration frequency of the SLGS is investigated. The Winkler-type, Pasternak-type, Visco-Winkler and Visco-Pasternak models are employed to simulate the interaction of the graphene sheets with a surrounding elastic medium. DQM is being used for the numerical solutions of the associated governing differential equations. The effects of (a) shear in-plane load, (b) small scale parameter, (c) elastic and viscoelastic medium, (d) aspect ratio, (e) boundary conditions and (f) material properties on the vibration frequency of SLGS are examined. The present work would be helpful while designing NEMS/MEMS devices using graphene sheets.

2 NONLOCAL PLATE MODELS

Nonlocal continuum theory states that the stress at a reference point x in an elastic continuum depends not only on strain at x but also on the strains at all other points x' in the body [22,23]. The basic equations for a linear homogenous elastic body using nonlocal elasticity theory are

$$\sigma_{ij} + f_i = \rho \ddot{u}_i \tag{1}$$

$$\sigma_{ij}(x) = \int \lambda\left(\left|x - x'\right|, \mu\right) C_{ijkl}\varepsilon_{kl}(x')dV(x'), \forall x \in V, \tag{2}$$

where σ_{ij}, f, ρ and u_i are the nonlocal elasticity stress tensor, mass density, body forces, and the displacement vector at point x, respectively. C_{ijkl} is the local stress tensor at any point x' in the body which is related to the strain tensor ε_{kl}. $\lambda\left(\left|x - x'\right|, \eta\right)$, $\left|x - x'\right|$ and $\mu = \left(e_0 l_i / a\right)$ are the nonlocal kernel function, Euclidean distance, and material constant that depends on the internal characteristic length l_i (such as the C-C bond length, lattice parameter) and external characteristic length a (like grapheme sheet length, wave length, crack length), respectively. The parameter e_0 is Eringen's nonlocal elasticity constant suitable to each material. The aforementioned integro-partial differential equations Eq. (1) based on nonlocal elasticity with that kernel function can be simplified to [16]

$$\left(1 - \left(e_0 l_i\right)^2 \nabla^2\right)\sigma^{nl} = C : \varepsilon \tag{3}$$

where ":" represents the double dot product. ∇^2 is the Laplacian operator and is given by $\nabla^2 = (\partial^2 / \partial x^2 + \partial^2 / \partial y^2)$. The classical plate theory (CPT) is used in present formulation. The CPT is based on assumptions similar to those used in thin beam or Euler-Bernoulli beam theory. The following assumptions are made in thin or classical plate theory [39]

1. The thickness of the plate (h) is small compared to its lateral dimensions.
2. The middle plane of plate does not undergo in-plane deformation. Thus, the mid-plane remains as the neutral plane after deformation or bending.
3. The displacement components of the mid-surface of the plate are small compared to the thickness of the plate.
4. The influence of transverse shear deformation is neglected. This implies that plane section normal to the mid-surface before deformation remains normal to the mid-surface even after deformation or bending. This assumption implies that the transverse shear strain ε_{xz} and ε_{yz} are negligible, where z denotes the thickness direction.
5. The transverse normal strain ε_{zz} under transverse loading can be neglected. The transverse normal stress σ_{zz} is small and hence can be neglected compared to the other components of stress.

On the basis of CPT, the two-dimensional forms the stress–strain relations are written as [15]

$$\begin{Bmatrix} \sigma_{xx}^{nl} \\ \sigma_{yy}^{nl} \\ \sigma_{xy}^{nl} \end{Bmatrix} - (e_0 l_i)^2 \nabla^2 \begin{Bmatrix} \sigma_{xx}^{nl} \\ \sigma_{yy}^{nl} \\ \sigma_{xy}^{nl} \end{Bmatrix} = \begin{bmatrix} E_1/(1-\upsilon_{12}\upsilon_{21}) & \upsilon_{12}E_2/(1-\upsilon_{12}\upsilon_{21}) & 0 \\ \upsilon_{12}E_2/(1-\upsilon_{12}\upsilon_{21}) & E_2/(1-\upsilon_{12}\upsilon_{21}) & 0 \\ 0 & 0 & 2G_{12} \end{bmatrix} \begin{Bmatrix} \varepsilon_{xx} \\ \varepsilon_{yy} \\ \varepsilon_{xy} \end{Bmatrix} \tag{4}$$

where E_1 and E_2 are Young's modulus, G_{12} is shear modulus, and υ_{12}, υ_{21} are Poisson's ratios, respectively. σ_{xx}^{nl}, σ_{yy}^{nl} and σ_{xy}^{nl} represent the nonlocal stress tensors. The strains in terms of displacement components in the middle surface can be written [39]

$$\varepsilon_{xx} = \frac{\partial u_0}{\partial x} - z\frac{\partial^2 w}{\partial x^2}, \varepsilon_{yy} = \frac{\partial v_0}{\partial y} - z\frac{\partial^2 w}{\partial y^2}, \varepsilon_{xy} = \frac{1}{2}\left(\left(\frac{\partial u_0}{\partial y} + \frac{\partial v_0}{\partial x}\right) - 2\frac{\partial^2 w}{\partial x \partial y}\right) \tag{5}$$

where u_0 and v_0 are the displacement of the middle surface of the plate at the point $(x, y, 0)$. In the foregoing, the first terms on the right-hand sides of the above equations represent the strain components in the middle surface due to its stretching, and terms with w represent the strain components due to bending. Stress resultants are defined as below [16]

$$N_{xx}=\int_{-h/2}^{h/2}\sigma_{xx}^{nl}dz\ ,\ N_{yy}=\int_{-h/2}^{h/2}\sigma_{yy}^{nl}dz\ ,\ N_{xy}=\int_{-h/2}^{h/2}\sigma_{xy}^{nl}dz\ ,$$
$$M_{xx}=\int_{-h/2}^{h/2}z\sigma_{xx}^{nl}dz\ ,\ M_{yy}=\int_{-h/2}^{h/2}z\sigma_{yy}^{nl}dz\ ,\ M_{xy}=\int_{-h/2}^{h/2}z\sigma_{xy}^{nl}dz \tag{6}$$

Here h denotes the thickness of the plate. By inserting Eq.(4), and Eq.(5) into Eq.(6) we can express stress resultants in terms of lateral deflection on the classical plate theory as follows [16]

$$M_{xx}-(e_0l_i)^2\nabla^2M_{xx}=-D_{11}\frac{\partial^2w}{\partial x^2}-D_{12}\frac{\partial^2w}{\partial y^2}\ ,\ M_{yy}-(e_0l_i)^2\nabla^2M_{yy}=-D_{12}\frac{\partial^2w}{\partial y^2}-D_{22}\frac{\partial^2w}{\partial x^2}$$
$$M_{xy}-(e_0l_i)^2\nabla^2M_{xy}=-2D_{66}\frac{\partial^2w}{\partial x\partial y}, \tag{7}$$

D_{ij} is known as the different flexural rigidity of the orthotropic rectangular nanoplte and are defined as [16]

$$\left(D_{11},\ D_{12},\ D_{22},\ D_{66}\right)=\int_{-h/2}^{h/2}\left(E_1/(1-\upsilon_{12}\upsilon_{21}),\ \upsilon_{12}E_2/(1-\upsilon_{12}\upsilon_{21}),\ E_2/(1-\upsilon_{12}\upsilon_{21}),\ G_{12}\right)z^2dz \tag{8}$$

Principle of virtual work is independent of constitutive relations. So this can be applied to derive the equilibrium equations of the nonlocal plates. Using the principle of virtual work, following equilibrium equation can be obtained [16]

$$\frac{\partial^2M_{xx}}{\partial x^2}+2\frac{\partial^2M_{xy}}{\partial x\partial y}+\frac{\partial^2M_{yy}}{\partial y^2}+q+\frac{\partial}{\partial x}\left(N_{xx}\frac{\partial w}{\partial x}+N_{xy}\frac{\partial w}{\partial y}\right)+\frac{\partial}{\partial y}\left(N_{yy}\frac{\partial w}{\partial y}+N_{xy}\frac{\partial w}{\partial x}\right)$$
$$=\rho h\frac{\partial^2w}{\partial t^2}+K_Ww-K_G\left(\frac{\partial^2w}{\partial x^2}+\frac{\partial^2w}{\partial y^2}\right)+C_d\frac{\partial w}{\partial t}. \tag{9}$$

A mono-layered rectangular graphene sheet embedded in a Visco-Pasternak foundation is shown in Fig.1, in which geometrical parameters of length a, width b and thickness h are also indicated. K_W indicate the Winkler modulus, K_G is the shear modulus of the surrounding elastic medium and C_d is damper modulus parameter. Here, ρ is density of nanoplate and q is the transverse force per unit area. In the present study, it is assumed that the nanoplate is free from any transverse loadings $(q=0)$. We consider the following relations for the vibration analysis under shear in-plane load.

$$N_{xx}=N_{yy}=0,\quad N_{xy}=P \tag{10}$$

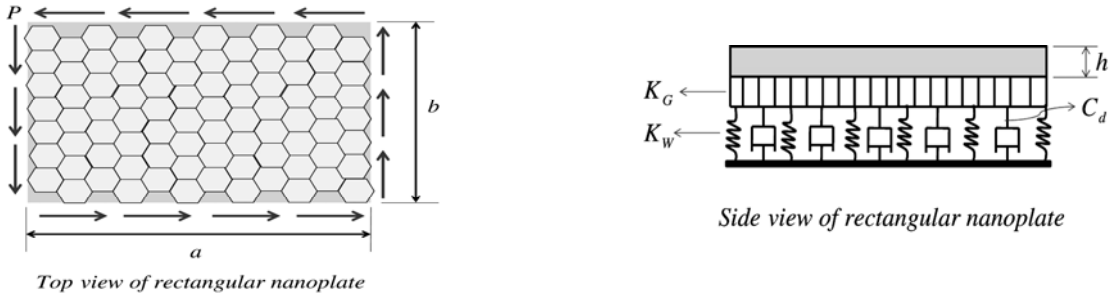

Fig. 1
Rectangular nanoplate embedded on a Visco-Pasternak foundation.

Substituting Eq. (7) and (10) into Eq. (9) one can obtain the following nonlocal governing differential equation for the vibration analysis of graphene sheets under shear in-plane loading

$$\begin{aligned}
&D_{11}\frac{\partial^4 w}{\partial x^4}+2(D_{12}+2D_{66})\frac{\partial^4 w}{\partial x^2\partial y^2}+D_{22}\frac{\partial^4 w}{\partial y^4}\\
&-K_G\left\{\left(\frac{\partial^2 w}{\partial x^2}+\frac{\partial^2 w}{\partial y^2}\right)-(e_0 l_i)^2\left(\frac{\partial^4 w}{\partial x^4}+2\frac{\partial^4 w}{\partial x^2\partial y^2}+\frac{\partial^4 w}{\partial y^4}\right)\right\}\\
&-K_W\left\{(e_0 l_i)^2\left(\frac{\partial^2 w}{\partial x^2}+\frac{\partial^2 w}{\partial y^2}\right)-w\right\}-C_d\left\{(e_0 l_i)^2\left(\frac{\partial^3 w}{\partial x^2\partial t}+\frac{\partial^3 w}{\partial y^2\partial t}\right)-\frac{\partial w}{\partial t}\right\}\\
&-2P\left\{\frac{\partial^2 w}{\partial x\partial y}-(e_0 l_i)^2\left(\frac{\partial^4 w}{\partial x^3\partial y}+\frac{\partial^4 w}{\partial x\partial y^3}\right)\right\}+\rho h\frac{\partial^2 w}{\partial t^2}-\rho h(e_0 l_i)^2\left(\frac{\partial^4 w}{\partial t^2\partial x^2}+\frac{\partial^4 w}{\partial t^2\partial y^2}\right)=0
\end{aligned} \tag{11}$$

Eq.(11) is the consistent fundamental equations for the nonlocal plate model for the shear buckling of orthotropic rectangular nanoplate. It should be noted that when the nonlocal scale coefficient $(e_0 l_i = 0)$, the Eqs. (4), (7) and (11) reduces to those of classical mechanics. The normal vibrations are harmonic, therefore the deflection in normal vibrations of thin plate can be expressed as:

$$w(x,y,t)=W^*(x,y)e^{i\omega_n t} \tag{12}$$

where ω_n is the natural frequency and $i^2=-1$. Substitution of Eq. (12) into Eq. (11) yields a four order partial differential equation involving natural mode $W^*(x,y)$

$$\begin{aligned}
&D_{11}\frac{\partial^4 W^*}{\partial x^4}+2(D_{12}+2D_{66})\frac{\partial^4 W^*}{\partial x^2\partial y^2}+D_{22}\frac{\partial^4 W^*}{\partial y^4}\\
&-K_G\left\{\left(\frac{\partial^2 W^*}{\partial x^2}+\frac{\partial^2 W^*}{\partial y^2}\right)-(e_0 l_i)^2\left(\frac{\partial^4 W^*}{\partial x^4}+2\frac{\partial^4 W^*}{\partial x^2\partial y^2}+\frac{\partial^4 W^*}{\partial y^4}\right)\right\}\\
&-K_W\left\{(e_0 l_i)^2\left(\frac{\partial^2 W^*}{\partial x^2}+\frac{\partial^2 W^*}{\partial y^2}\right)-W^*\right\}-C_d\left\{(e_0 l_i)^2\left(\frac{\partial^3 W^*}{\partial x^2\partial t}+\frac{\partial^3 W^*}{\partial y^2\partial t}\right)-\frac{\partial W^*}{\partial t}\right\}\\
&-2P\left\{\frac{\partial^2 W^*}{\partial x\partial y}-(e_0 l_i)^2\left(\frac{\partial^4 W^*}{\partial x^3\partial y}+\frac{\partial^4 W^*}{\partial x\partial y^3}\right)\right\}\\
&-\rho h\omega_n^2 W^*+\rho h(e_0 l_i)^2\omega_n^2\left(\frac{\partial^2 W^*}{\partial x^2}+\frac{\partial^2 W^*}{\partial y^2}\right)=0
\end{aligned} \tag{13}$$

3 SOLUTION BY DIFFERNTIAL QUADRATURE METHOD

DQM has been found to be an efficient numerical technique for the solution of initial and boundary value problems [41-49]. Since DQ technique provides simple formulation and low computational cost, it has been widely used for the analysis of mechanical behaviors of the structural elements at large scale, such as dynamic and stability problems. In recent years, many researchers used DQ approach in solving the governing equations of nanostructures. Mohammadi et al. [37] applied new version of DQM for vibration analysis of embedded single-layer circular nanoplate. Farajpour et al. [41] used DQM for the buckling of orthotropic micro/nanoscale plate under linearly varing in-plane load. Danesh et al. [42] used DQM for the vibration analysis of tapered nanorod with different

boundary conditions. Consider a two dimensional field variable $u(x,y)$, the m-th order derivative of it with respect to x, and the $(m+n)-th$ order derivative of it with respect to x and y is approximated as [47]

$$\left.\frac{\partial^m u}{\partial x^m}\right|_{(x_i,y_i)} = \sum_{k=1}^{N} C_{ik}^{(m)} u(x_k, y_j, t) = \sum_{k=1}^{N} C_{ik}^{(m)} u_{kj}(t) \tag{14a}$$

$$\left.\frac{\partial^{(m+n)} u}{\partial x^m \partial y^n}\right|_{(x_i,y_i)} = \sum_{k=1}^{N} C_{ik}^{(m)} \overline{C}_{jl}^{(n)} u(x_k, y_l, t) = \sum_{k=1}^{N} C_{ik}^{(m)} \overline{C}_{jl}^{(n)} u_{kl}(t) \tag{14b}$$

The method developed by Shu and Richard [46] is claimed to be computationally more accurate than other methods [45]. According to Shu and Richard rule [46], the weighting coefficients of the first-order derivatives in ζ direction ($\zeta = x$ or y) are determined as [47]

$$C_{ij}^{(1)} = \begin{cases} \dfrac{M(\zeta_i)}{(\zeta_i - \zeta_j) M(\zeta_j)} & \text{for } i \neq j \\ -\sum\limits_{j=1, i\neq j}^{N} C_{ij}^{(1)} & \text{for } i = j \end{cases} \qquad i,j=1,2,...,N \tag{15}$$

where

$$M(\zeta_i) = \prod_{j=1, i\neq j}^{N} (\zeta_i - \zeta_j) \tag{16}$$

In order to evaluate the weighting coefficients of higher-order derivatives, recurrence relations are derived as [47]

$$C_{ij}^{(r)} = r\left[C_{ij}^{(r-1)} C_{ij}^{(1)} - \frac{C_{ij}^{(r-1)}}{(\zeta_i - \zeta_j)} \right] \quad for\ i, j = 1,2,...,N,\ i \neq j\ and\ 2 \le r \le N-1 \tag{17}$$

$$C_{ii}^{(r)} = -\sum_{j=1,\ i\neq j}^{N} C_{ij}^{(r)} \quad for\ i = 1,2,...,N\ and\ 1 \le r \le N-1 \tag{18}$$

The natural and simplest choice of the grid points is equally spaced points in the direction of the coordinate axes of the computational domain. It was demonstrated that non-uniform grid points gives a better results with the same number of equally spaced grid points. In this paper, we choose these set of grid points in terms of natural coordinate directions ξ and η as [47]

$$\begin{aligned} \xi_i &= \frac{1}{2}\left(1 - \cos\left(\frac{(i-1)\pi}{(N-1)}\right)\right) \qquad for\ \ i = 1, 2, \ldots, N \\ \eta_j &= \frac{1}{2}\left(1 - \cos\left(\frac{(j-1)\pi}{(M-1)}\right)\right) \qquad for\ \ j = 1, 2, \ldots, M \end{aligned} \tag{19}$$

A rectangular grapheme sheet is considered to be embedded in an elastic medium. The geometric properties of the grapheme sheet are denoted by length *a,* width *b,* thickness *h*. For convenience and generality, we introduce the following non-dimensional parameters

$$W = \frac{W^*}{a},\ \xi = \frac{x}{a},\ \eta = \frac{y}{b},\ \psi = \frac{e_0 l_i}{a},\ \beta = \frac{a}{b},\ \overline{\mathrm{K}}_W = \frac{K_W a^4}{D_{11}}, \overline{\mathrm{K}}_G = \frac{K_G a^2}{D_{11}}, \overline{\mathrm{P}} = \frac{Pa^2}{D_{11}},$$
$$\lambda_1 = \frac{D_{12} + 2D_{66}}{D_{11}},\ \lambda_2 = \frac{D_{22}}{D_{11}},\ \overline{\mathrm{C}}_d = \frac{C_d a^2}{\sqrt{\rho h D}},\ \tau = \frac{t}{a^2}\sqrt{\frac{D}{\rho h}}, \Omega^2 = \frac{\rho h \omega^2 a^4}{D_{11}}. \tag{20}$$

Using the above expressions, a non-dimensional nonlocal differential equation for vibration of rectangular grapheme sheet under shear in-plane load can be obtained

$$\begin{aligned}
&\left\{\sum_{k=1}^{N} C_{ik}^{(4)} W_{k,j} + 2\lambda_1\beta^2 \sum_{k1=1}^{N}\sum_{K2=1}^{M} C_{i,k1}^{(2)} \overline{C}_{j,k2}^{(2)} W_{k1,k2} + \lambda_2\beta^4 \sum_{k=1}^{M} \overline{C}_{jk}^{(4)} W_{i,k}\right\} \\
&-\overline{\mathrm{K}}_G \left\{\begin{array}{l} \sum_{k=1}^{N} C_{ik}^{(2)} W_{k,j} + \beta^2 \sum_{k=1}^{M} \overline{C}_{jk}^{(2)} W_{i,j} \\ -\psi^2 \left\{\sum_{k=1}^{N} C_{ik}^{(4)} W_{k,j} + 2\beta^2 \sum_{k1=1}^{N}\sum_{K2=1}^{M} C_{i,k1}^{(2)} \overline{C}_{j,k2}^{(2)} W_{k1,k2} + \beta^4 \sum_{k=1}^{M} \overline{C}_{jk}^{(4)} W_{i,k}\right\} \end{array}\right\} \\
&+\overline{K}_W \left\{W_{i,j} - \psi^2 \left\{\sum_{k=1}^{N} C_{ik}^{(2)} W_{k,j} + \beta^2 \sum_{k=1}^{M} \overline{C}_{jk}^{(2)} W_{i,j}\right\}\right\} + \overline{C}_d \omega i \left\{W_{i,j} - \psi^2 \left\{\sum_{k=1}^{N} C_{ik}^{(2)} W_{k,j} + \beta^2 \sum_{k=1}^{M} \overline{C}_{jk}^{(2)} W_{i,j}\right\}\right\} \\
&-2\overline{P} \left\{\begin{array}{l} \beta \sum_{k1=1}^{N}\sum_{k2=1}^{M} C_{i,k1}^{(1)} \overline{C}_{j,k2}^{(1)} W_{k1,k2} \\ -\psi^2 \beta \left\{\sum_{k1=1}^{N}\sum_{k2=1}^{M} C_{i,k1}^{(3)} \overline{C}_{j,k2}^{(1)} W_{k1,k2} + \beta^2 \sum_{k1=1}^{N}\sum_{k2=1}^{M} C_{i,k1}^{(1)} \overline{C}_{j,k2}^{(3)} W_{k1,k2}\right\} \end{array}\right\} \\
&-\Omega^2 \left\{W_{i,j} - \psi^2 \left\{\sum_{k=1}^{N} C_{ik}^{(2)} W_{k,j} + \beta^2 \sum_{k=1}^{M} \overline{C}_{jk}^{(2)} W_{i,j}\right\}\right\} = 0
\end{aligned} \tag{21}$$

C and $\overline{C}$ are the weighting coefficient matrix in the *x*, *y* directions respectively, Eq.(21) is applied at the interior points, $2 \le i \le N-1,\ 2 \le j \le M-1$ and only the Dirichlet condition $(W = 0)$ is implemented. So Eq. (21) can be obtained [47]

$$\begin{aligned}
&\left\{\sum_{k=2}^{N-1} C_{ik}^{(4)} W_{k,j} + 2\lambda_1\beta^2 \sum_{k1=2}^{N-1}\sum_{K2=2}^{M-1} C_{i,k1}^{(2)} \overline{C}_{j,k2}^{(2)} W_{k1,k2} + \lambda_2\beta^4 \sum_{k=2}^{M-1} \overline{C}_{jk}^{(4)} W_{i,k}\right\} \\
&-\overline{\mathrm{K}}_G \left\{\begin{array}{l} \sum_{k=2}^{N-1} C_{ik}^{(2)} W_{k,j} + \beta^2 \sum_{k=2}^{M-1} \overline{C}_{jk}^{(2)} W_{i,j} \\ -\psi^2 \left\{\sum_{k=2}^{N-1} C_{ik}^{(4)} W_{k,j} + 2\beta^2 \sum_{k1=2}^{N-1}\sum_{K2=2}^{M-1} C_{i,k1}^{(2)} \overline{C}_{j,k2}^{(2)} W_{k1,k2} + \beta^4 \sum_{k=2}^{M-1} \overline{C}_{jk}^{(4)} W_{i,k}\right\} \end{array}\right\} \\
&+\overline{K}_W \left\{W_{i,j} - \psi^2 \left\{\sum_{k=2}^{N-1} C_{ik}^{(2)} W_{k,j} + \beta^2 \sum_{k=2}^{M-1} \overline{C}_{jk}^{(2)} W_{i,j}\right\}\right\} + \overline{C}_d \omega i \left\{W_{i,j} - \psi^2 \left\{\sum_{k=2}^{N-1} C_{ik}^{(2)} W_{k,j} + \beta^2 \sum_{k=2}^{M-1} \overline{C}_{jk}^{(2)} W_{i,j}\right\}\right\} \\
&-2\overline{P} \left\{\begin{array}{l} \beta \sum_{k1=2}^{N-1}\sum_{k2=2}^{M-1} C_{i,k1}^{(1)} \overline{C}_{j,k2}^{(1)} W_{k1,k2} \\ -\psi^2 \beta \left\{\sum_{k1=2}^{N-1}\sum_{k2=2}^{M-1} C_{i,k1}^{(3)} \overline{C}_{j,k2}^{(1)} W_{k1,k2} + \beta^2 \sum_{k1=2}^{N-1}\sum_{k2=2}^{M-1} C_{i,k1}^{(1)} \overline{C}_{j,k2}^{(3)} W_{k1,k2}\right\} \end{array}\right\} \\
&-\Omega^2 \left\{W_{i,j} - \psi^2 \left\{\sum_{k=2}^{N-1} C_{ik}^{(2)} W_{k,j} + \beta^2 \sum_{k=2}^{M-1} \overline{C}_{jk}^{(2)} W_{i,j}\right\}\right\} = 0
\end{aligned} \tag{22}$$

The idea of this approach is the same as that for the beam that it presented by Shu [47] to implement the simply supported and clamped conditions. The derivatives in the boundary condition are also discretized by the DQ method. The discrete form of any combination of the clamped and simply supported conditions can be written as [47]

$$W_{1,j}=0,\ W_{N,j}=0,\ W_{i,1}=0,\ W_{i,M}=0 \tag{23}$$

at all boundary points

$$\sum_{k=1}^{N} C_{1,k}^{(n0)} W_{k,j}=0 \quad \text{at } \zeta=0 \tag{24}$$

$$\sum_{k=1}^{N} C_{N,k}^{(n1)} W_{k,j}=0 \quad \text{at } \zeta=1 \tag{25}$$

$$\sum_{k=1}^{M} C_{i,k}^{(m0)} W_{i,k}=0 \quad \text{at } \eta=0 \tag{26}$$

$$\sum_{k=1}^{M} C_{M,k}^{(m1)} W_{i,k}=0 \quad \text{at } \eta=1 \tag{27}$$

where n0, n1, m0 and m1 are taken as either 1 or 2: 1 is used for the clamp edge condition and 2 is used for simply supported boundary condition. n0, n1, m0 and m1 correspond to the edge of $\xi=0,\ \xi=1,\ \eta=0$ and $\eta=1$ respectively. It is noted that Eq.(23) corresponds to Dirichlet boundary condition at the four edges of the plate, and Eqs.(24-27) result from the derivative boundary conditions. Obviously, Eq.(23) can be easily substituted into Eq. (22).However, Eqs.(24-27) cannot be directly substituted into Eq.(21). This difficulty can be easily overcome. Using the same procedure as for the beam [47]. Eqs. (24-25) can be coupled to give two solutions $W_{2,j}$ and $W_{N-1,j}$ [47].

$$W_{2,J}=\frac{1}{AXN}\sum_{k=3}^{N-2} AXK1\ W_{k,J} \qquad for\ \mathrm{j}=3,\ 4,\ \ldots,\ \mathrm{M}-2 \tag{28}$$

$$W_{N-1,J}=\frac{1}{AXN}\sum_{k=3}^{N-2} AXKN\ W_{k,J} \qquad for\ \mathrm{j}=3,\ 4,\ \ldots,\ \mathrm{M}-2 \tag{29}$$

where

$$AXN=\ \mathrm{C}_{N,2}^{(n1)}\ \mathrm{C}_{1,N-1}^{(n0)}-C_{1,2}^{(n0)}\ \mathrm{C}_{N,N-1}^{(n1)} \tag{30}$$

$$AXK1=\ \mathrm{C}_{1,k}^{(n0)}\ \mathrm{C}_{N,N-1}^{(n1)}-C_{1,N-1}^{(n0)}\ \mathrm{C}_{N,k}^{(n1)} \tag{31}$$

$$AXKN=\ \mathrm{C}_{1,2}^{(n0)}\ \mathrm{C}_{N,k}^{(n1)}-C_{1,k}^{(n0)}\ \mathrm{C}_{N,2}^{(n1)} \tag{32}$$

Similarly Eq.(26) and Eq.(27) can be coupled to give two solutions $W_{i,2}$ and $W_{i,M-1}$ [47].

$$W_{i,2}=\frac{1}{AYM}\sum_{k=3}^{M-2} AYK1\ W_{i,k} \qquad for\ \mathrm{i}=3,\ 4,\ \ldots,\ \mathrm{N}-2 \tag{33}$$

$$W_{i,M-1}=\frac{1}{AYM}\sum_{k=3}^{M-2} AYKM\ W_{i,k} \qquad for\ \mathrm{i}=3,\ 4,\ \ldots,\ \mathrm{N}-2 \tag{34}$$

where

$$AYM=\ \overline{\mathrm{C}}_{M,2}^{(m1)}\ \overline{\mathrm{C}}_{1,M-1}^{(m0)}-\overline{C}_{1,2}^{(m0)}\ \overline{\mathrm{C}}_{M,M-1}^{(m1)} \tag{35}$$

$$AYK1=\ \overline{\mathrm{C}}_{1,k}^{(m0)}\ \overline{\mathrm{C}}_{M,M-1}^{(m1)}-\overline{C}_{1,M-1}^{(m0)}\ \overline{\mathrm{C}}_{M,k}^{(m1)} \tag{36}$$

$$AYKM=\ \overline{\mathrm{C}}_{1,2}^{(m0)}\ \overline{\mathrm{C}}_{M,k}^{(m1)}-\overline{C}_{1,k}^{(m0)}\ \overline{\mathrm{C}}_{M,2}^{(m1)} \tag{37}$$

For the point near the four corners, the four Eqs. (24-27) have to be coupled to provide the flowing four solutions[47]

$$W_{2,2} = \frac{1}{AXN}\frac{1}{AYM}\sum_{k1=3}^{N-2}\sum_{k2=3}^{M-2} AXK1\ \mathrm{AYK1}\ \mathrm{W}_{k1,k2} \tag{38}$$

$$W_{N-1,2} = \frac{1}{AXN}\frac{1}{AYM}\sum_{k1=3}^{N-2}\sum_{k2=3}^{M-2} AXKN\ \mathrm{AYK1}\ \mathrm{W}_{k1,k2} \tag{39}$$

$$W_{2,M-1} = \frac{1}{AXN}\frac{1}{AYM}\sum_{k1=3}^{N-2}\sum_{k2=3}^{M-2} AXK1\ \mathrm{AYKM}\ \mathrm{W}_{k1,k2} \tag{40}$$

$$W_{N-1,M-1} = \frac{1}{AXN}\frac{1}{AYM}\sum_{k1=3}^{N-2}\sum_{k2=3}^{M-2} AXKN\ \mathrm{AYKM}\ \mathrm{W}_{k1,k2} \tag{41}$$

For the Eqs. (38-41), the index k in the AXK1 and AXKN expressions is replaced by *k1*, and the index k in the AYK1 and AYKM expressions is replaced by *k2*. With Eqs. (23, 28, 29, 33, 34, 38-41), the entire boundary conditions can be directly substituted into Eq. (21). As a result, the final eigenvalue equation system becomes [47]

$$\left\{\sum_{k=3}^{N-2} C_1 W_{k,j} + \sum_{k1=3}^{N-2}\sum_{K2=3}^{M-2} C_2 W_{k1,k2} + \sum_{k=3}^{M-2} C_3 W_{i,k}\right\} - \Omega^2\left\{W_{i,j} - \psi^2\left\{\sum_{k=3}^{N-2} C_4 W_{k,j} + \beta^2\sum_{k=3}^{M-2} C_5 W_{i,k}\right\}\right\} = 0 \tag{42}$$

where

$$\begin{aligned} C_1 = {} & \left(1+\bar{K}_G\psi^2\right)\left(C_{i,k}^{(4)} - \frac{C_{i,2}^{(4)}AXK1 + C_{i,N-1}^{(4)}AXKN}{AXN}\right) \\ & -\left(\bar{K}_G + \bar{K}_W\psi^2 + \bar{C}_d\psi^2\omega i\right)\left(C_{i,k}^{(2)} - \frac{C_{i,2}^{(2)}AXK1 + C_{i,N-1}^{(2)}AXKN}{AXN}\right) \end{aligned} \tag{43}$$

$$\begin{aligned} C_3 = {} & \left(\lambda_2\beta^4 + \bar{K}_G\beta^4\right)\left(\bar{C}_{j,k}^{(4)} - \frac{\bar{C}_{j,2}^{(4)}AYK1 + \bar{C}_{j,M-1}^{(4)}AYKM}{AYM}\right) - \\ & \left(\bar{K}_G\beta^2 + \bar{K}_W\beta^2\psi^2 + \bar{C}_d\beta^2\psi^2\omega i\right)\left(\bar{C}_{j,k}^{(2)} - \frac{\bar{C}_{j,2}^{(2)}AYK1 + \bar{C}_{j,M-1}^{(2)}AYKM}{AYM}\right) \end{aligned} \tag{44}$$

$$C_4 = \left(C_{i,k}^{(2)} - \frac{C_{i,2}^{(2)}AXK1 + C_{i,N-1}^{(2)}AXKN}{AXN}\right) \tag{45}$$

$$C_5 = \left(\bar{C}_{j,k}^{(2)} - \frac{\bar{C}_{j,2}^{(2)}AYK1 + \bar{C}_{j,M-1}^{(2)}AYKM}{AYM}\right) \tag{46}$$

$$C_2=\left(2\lambda_1\beta^2+2\bar{K}_G\beta^2\psi^2\right)\left(\begin{array}{l} C^{(2)}_{i,k1}\bar{C}^{(2)}_{j,k2}-\dfrac{\left(AXK1\ \mathrm{C}^{(2)}_{i,2}+AXKN\ \mathrm{C}^{(2)}_{i,N-1}\right)}{AXN}\bar{C}^{(2)}_{j,k2}- \\ \dfrac{\left(AYK1\ \bar{\mathrm{C}}^{(2)}_{j,2}+AYKM\ \bar{\mathrm{C}}^{(2)}_{j,M-1}\right)}{AYM}C^{(2)}_{i,k1}+ \\ \dfrac{\left(AYK1AXK1\ \mathrm{C}^{(2)}_{i,2}\ \bar{\mathrm{C}}^{(2)}_{j,2}+AYKMAXKN\ \mathrm{C}^{(2)}_{i,N-1}\ \bar{\mathrm{C}}^{(2)}_{j,2}\right)}{AYM\ AXN}+ \\ \dfrac{\left(AYK1AXK1\ \mathrm{C}^{(2)}_{i,2}\ \bar{\mathrm{C}}^{(2)}_{j,M-1}+AYKMAXKN\ \mathrm{C}^{(2)}_{i,N-1}\ \bar{\mathrm{C}}^{(2)}_{j,M-1}\right)}{AYM\ AXN} \end{array}\right)-$$

$$\left(2\bar{P}\beta\right)\left(\begin{array}{l} C^{(1)}_{i,k1}\bar{C}^{(1)}_{j,k2}-\dfrac{\left(AXK1\ \mathrm{C}^{(1)}_{i,2}+AXKN\ \mathrm{C}^{(1)}_{i,N-1}\right)}{AXN}\bar{C}^{(1)}_{j,k2}- \\ \dfrac{\left(AYK1\ \bar{\mathrm{C}}^{(1)}_{j,2}+AYKM\ \bar{\mathrm{C}}^{(1)}_{j,M-1}\right)}{AYM}C^{(1)}_{i,k1}+ \\ \dfrac{\left(AYK1AXK1\ \mathrm{C}^{(1)}_{i,2}\ \bar{\mathrm{C}}^{(1)}_{j,2}+AYKMAXKN\ \mathrm{C}^{(1)}_{i,N-1}\ \bar{\mathrm{C}}^{(1)}_{j,2}\right)}{AYM\ AXN}+ \\ \dfrac{\left(AYK1AXK1\ \mathrm{C}^{(1)}_{i,2}\ \bar{\mathrm{C}}^{(1)}_{j,M-1}+AYKMAXKN\ \mathrm{C}^{(1)}_{i,N-1}\ \bar{\mathrm{C}}^{(1)}_{j,M-1}\right)}{AYM\ AXN} \end{array}\right)+$$

$$\left(2\bar{P}\psi^2\beta\right)\left(\begin{array}{l} C^{(3)}_{i,k1}\bar{C}^{(1)}_{j,k2}-\dfrac{\left(AXK1\ \mathrm{C}^{(3)}_{i,2}+AXKN\ \mathrm{C}^{(3)}_{i,N-1}\right)}{AXN}\bar{C}^{(1)}_{j,k2}- \\ \dfrac{\left(AYK1\ \bar{\mathrm{C}}^{(1)}_{j,2}+AYKM\ \bar{\mathrm{C}}^{(1)}_{j,M-1}\right)}{AYM}C^{(3)}_{i,k1}+ \\ \dfrac{\left(AYK1AXK1\ \mathrm{C}^{(3)}_{i,2}\ \bar{\mathrm{C}}^{(1)}_{j,2}+AYKMAXKN\ \mathrm{C}^{(3)}_{i,N-1}\ \bar{\mathrm{C}}^{(1)}_{j,2}\right)}{AYM\ AXN}+ \\ \dfrac{\left(AYK1AXK1\ \mathrm{C}^{(3)}_{i,2}\ \bar{\mathrm{C}}^{(1)}_{j,M-1}+AYKMAXKN\ \mathrm{C}^{(3)}_{i,N-1}\ \bar{\mathrm{C}}^{(1)}_{j,M-1}\right)}{AYM\ AXN} \end{array}\right)+$$

$$\left(2\bar{P}\psi^2\beta^3\right)\left(\begin{array}{l} C^{(1)}_{i,k1}\bar{C}^{(3)}_{j,k2}-\dfrac{\left(AXK1\ \mathrm{C}^{(1)}_{i,2}+AXKN\ \mathrm{C}^{(1)}_{i,N-1}\right)}{AXN}\bar{C}^{(3)}_{j,k2}- \\ \dfrac{\left(AYK1\ \bar{\mathrm{C}}^{(3)}_{j,2}+AYKM\ \bar{\mathrm{C}}^{(3)}_{j,M-1}\right)}{AYM}C^{(1)}_{i,k1}+ \\ \dfrac{\left(AYK1AXK1\ \mathrm{C}^{(1)}_{i,2}\ \bar{\mathrm{C}}^{(3)}_{j,2}+AYKMAXKN\ \mathrm{C}^{(1)}_{i,N-1}\ \bar{\mathrm{C}}^{(3)}_{j,2}\right)}{AYM\ AXN}+ \\ \dfrac{\left(AYK1AXK1\ \mathrm{C}^{(1)}_{i,2}\ \bar{\mathrm{C}}^{(3)}_{j,M-1}+AYKMAXKN\ \mathrm{C}^{(1)}_{i,N-1}\ \bar{\mathrm{C}}^{(3)}_{j,M-1}\right)}{AYM\ AXN} \end{array}\right) \tag{47}$$

Since Eq.(42) has $(N-4)\times(M-4)$ unknowns, it should be applied at $(N-4)\times(M-4)$ interior points to close the system. This can be done by applying it at the interior points, $3\le i\le N-2,\ 3\le j\le M-2$.

After implementation of the boundary conditions, Eq. (42) can be written in matrix form as [44]

$$\left([K]+\omega[C]+\omega^2[M]\right)\begin{Bmatrix} d_b \\ d_d \end{Bmatrix}=0 \tag{48}$$

where the subscript *b* stands for the elements related to the boundary points while subscript *d* is associated with the remain-der elements. The $[K]$, $[C]$ and $[M]$ are the stiffness, damping and mass matrixes, respectively. For solving

the Eq.(39) and reducing it to the standard form of eigenvalue problem, it is convenient to rewrite Eq.(39) as the following first order variable as [44]

$$\{\dot{Z}\} = [A]\{Z\} \tag{49}$$

In which, the state vector Z and state matrix $[A]$ are defined as [44]

$$Z = \begin{Bmatrix} d_d \\ \dot{d}_d \end{Bmatrix} \text{ and } A = \begin{bmatrix} [0] & [I] \\ -[M^{-1}K] & -[M^{-1}C] \end{bmatrix} \tag{50}$$

where $[0]$ and $[I]$ are the zero and unitary matrices, respectively. However, the frequencies obtained from the solution of Eq.(42) are complex due to the damping. Hence, the results are containing two real and imaginary parts. The imaginary part is corresponding to the system damping and the real part representing the system natural frequencies [44]. Fig. 2 shows the flowchart of steps of DQ method.

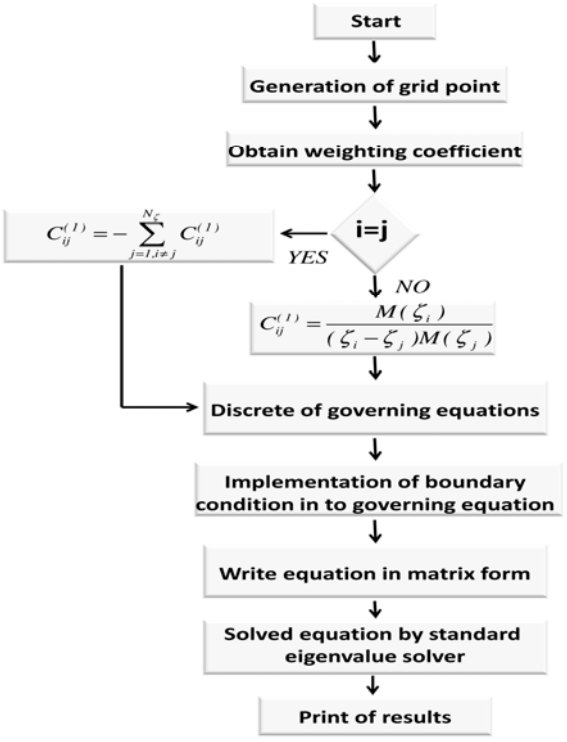

Fig. 2
Flowchart of steps of applied DQ method.

4 SOLUTION BY GALERKIN METHOD

In this section, Galerkin method is used to solve the governing Eq. (13). The Galerkin approach is an efficient and powerful numerical method for the solution of the differential equations. Since this numerical solution technique provides simple formulation and low computational cost, it has been widely used for the analysis of mechanical behavior of the structural elements at large scale, such as static, dynamic and stability problems. The Galerkin method was used by Romeo and Frulla [50] to study the postbuckling behavior of stiffened composite panels under biaxial compressive load. Saadatpour and Azhari [51] used Galerkin technique for static analysis of simply

supported plates of arbitrary quadrilateral shape. Furthermore, recently, the Galerkin method was employed to investigate the size effects on the small-deflection stability of various quadrilateral nanoplates such as skew, rhombic and trapezoidal nanoplates [52].

We assume simply supported boundary conditions along all the four edges of the single-layered graphene sheet. The boundary conditions are mathematically written as:

$$W=0,\ \frac{\partial^2 W}{\partial \xi^2}=0 \ \text{ at } \xi=0 \text{ and } \xi=1 \qquad , \qquad W=0,\ \frac{\partial^2 W}{\partial \eta^2}=0 \ \text{ at } \eta=0 \text{ and } \eta=1 \tag{51}$$

Using the general procedure of the Galerkin method yields the following

$$\iint_{\Lambda} \Gamma\left(\sum_{m=1}^{M}\sum_{n=1}^{N} c_{nm} f_{nm}(\xi,\eta)\right) f_{ij}(\xi,\eta)\, d\Lambda = 0 \tag{52}$$

where $f_{ij}(x,y)$ represents basic functions. The chosen basic functions for the lateral deflection must satisfy all boundary conditions but not necessarily satisfy the governing Eq. (13). c_{nm} $(i=1,2,...,N;\ j=1,2,...,M)$ are $N\times M$ unknown coefficients to be determined. The integration extends over the entire domain of the nanoplate (Λ). The symbol Γ indicates a differential operator and is defined as follows

$$\begin{aligned}\Gamma(*) &= \Theta_1 \frac{\partial^4}{\partial \xi^4}(*) + \Theta_2 \frac{\partial^4}{\partial \xi^2 \partial \eta^2}(*) + \Theta_3 \frac{\partial^4}{\partial \eta^4}(*) + \Theta_4 \frac{\partial^4}{\partial \xi^3 \partial \eta}(*) + \Theta_5 \frac{\partial^4}{\partial \xi \partial \eta^3}(*) \\ &+ \Theta_6 \frac{\partial^2}{\partial \xi \partial \eta}(*) + \Theta_7 \frac{\partial^2}{\partial \xi^2}(*) + \Theta_8 \frac{\partial^2}{\partial \eta^2}(*) + \Theta_9 (*)\end{aligned} \tag{53}$$

Obviously, coefficients Θ_i $(i=1,2,..,9)$ can be obtained in the following form

$$\begin{aligned}&\Theta_1 = \left(1+\overline{\mathrm{K}}_G\psi^2\right),\ \Theta_2 = 2\beta^2\left(\lambda_1+\overline{\mathrm{K}}_G\psi^2\right),\ \Theta_3 = \beta^4\left(\lambda_2+\overline{\mathrm{K}}_G\psi^2\right),\ \Theta_4 = 2\overline{P}\psi^2\beta, \\ &\Theta_5 = 2\overline{P}\psi^2\beta^3 \Theta_6 = -2\overline{P}\beta,\ \Theta_7 = -\overline{\mathrm{K}}_W\psi^2 - \overline{\mathrm{C}}_d i\psi^2\omega - \overline{\mathrm{K}}_G + \Omega^2\psi^2, \\ &\Theta_8 = -\overline{\mathrm{K}}_W\beta^2\psi^2 - \overline{\mathrm{C}}_d\beta^2\psi^2 i\omega - \overline{\mathrm{K}}_G\beta^2 + \Omega^2\psi^2\beta^2,\ \Theta_9 = \overline{\mathrm{K}}_W + \overline{\mathrm{C}}_d i\omega - \Omega^2\end{aligned} \tag{54}$$

In the Galerkin method, the lateral deflection is described by a linear combination of the basic functions for the numerical solutions of the plate problem under investigation. The basic functions must satisfy all the above-mentioned boundary conditions. The chosen basic function for $W(\xi,\eta)$ are

$$f_{ij}(x,y) = \sin(i\pi\xi)\sin(j\pi\eta) \tag{55}$$

The above basic functions do not satisfy Eq. (13) but satisfy the prescribed boundary conditions given in Eq. (51) exactly. Note that the boundary conditions are incorporated in the analysis by direct substitution of Eq. (55) into Eq. (52).

After employing the aforementioned solution procedure, one obtains the following system of linear algebraic equations

$$\left([A]+\Omega^2[B]+\omega[D]\right)\{c\}=0 \tag{56}$$

where $[A],[B]$ and $[D]$ are the $(N\times M)\times(N\times M)$ square matrix. $\{c\}$ indicates the column matrix of unknown coefficients c_{ij}. The Galerkin method transforms the stability problem into a standard eigenvalue problem. The

buckling parameters $\left(\Omega^2\right)$ are the eigenvalues of Eq. (56) that can be found by using standard eigenvalue extraction techniques.

5 RESULTS AND DISCUSSION

In the following section, some numerical examples will be presented. The validity of the suggested model is checked by comparing the obtained results with those given in the literature. Moreover, the effects of the main parameters including the properties material of the graphene sheet, the shear and Winkler modulus factor, the nonlocal parameter, the boundary conditions, the aspect ratio, length of graphene sheet and shear in-plane load on the structural vibration frequency of the graphene sheet are also studied. The orthotropic material properties are taken as that of nano single-layered graphene sheets. The Young's moduli and Poisson's ratios are $E_1 = 1765$ Gpa, $E_2 = 1588$ Gpa, $\upsilon_{12} = 0.3$, $\upsilon_{21} = 0.27$ respectively [53]. Following six boundary conditions have been considered in the vibration analysis [34-37] of the orthotropic graphene sheets.

SSSS: All edges Simply Supported.
CCCC: All edges Clamped.
CCCS: Simply Supported along Y=*b* and Clamped along X=*a*, Y=0 and X=0.
CCSS: Simply Supported along Y=*b* and X=a and Clamped along X=0 and Y=0.
CSCS: Simply Supported along Y=0 and Y=*b* and Clamped along X=0 and X=*a*.
SSSC: Simply Supported along Y=0, Y=*b* and X=*a* and Clamped along X=0.
The relative percentage errors are measured in comparison with the Galerkin solutions.

$$\text{Re}\,lative\ \text{error}=\left|\frac{\Omega_{DQM}-\Omega_{Galerkin}}{\Omega_{Galerkin}}\right|\times 100$$

The variations of error of the present analysis versus different number of grid points are plotted in Fig.3. It is shown that by using eleven grid points, the error is less than 0.5%. Also, the stability of convergence behaviors of the solutions is confirmed. Here, also excellent agreement has been achieved for natural frequencies evaluated with only eleven grid points.

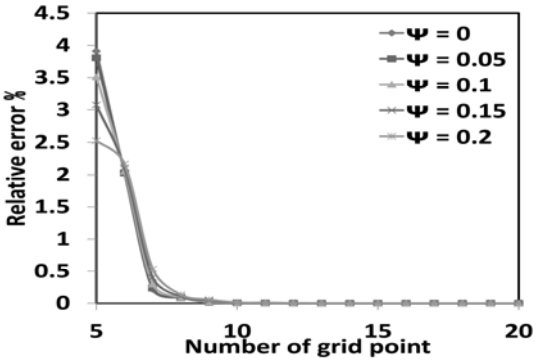

Fig. 3
The relative error of the fundamental frequency parameter of nanoplate with respect to increase in the number of grid points.

A computer code is developed in MATLAB based on Eq. (42). As DQ results are sensitive to lower grid points, a convergence test is performed to determine the minimum number of grid points required to obtain stable and accurate results for Eq. (42). According to Fig. 4, present solution is convergent. From the figure it is clearly seen that twelve number of grid points ($N = M = 12$) are sufficient to obtain the accurate solutions for the present analysis.

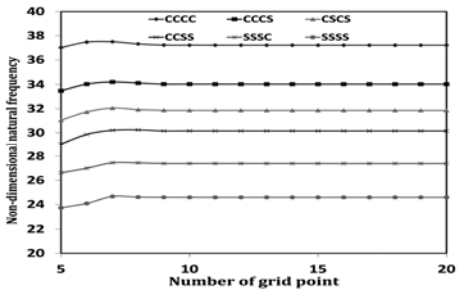

Fig. 4
Convergence study and minimum number of grid points ($N = M$) required to obtain accurate results for other boundary conditions ($K_W = 100, K_G = 10, \quad \psi = 0.1, \beta = 1$) .

Table 1
Comparison of critical shear load obtained from the present model with some known results available in the literature for a different aspect ratio and boundary conditions.

Boundary condition	Reference		a/b		
			1/1	1/2	1/3
All edges clamped	Budiansky and Connor [56]	Lower bounds	144.5	101.8	94.4
		Upper bounds	146	102.3	95.4
	Bassily and Dickinson [54]		144.716	101.276	94.364
	Present		144.5109	101.1436	94.0999
Edges length b clamped, edges length a simply supported	Cook and Rockey [55]		124.36	99.09	94.85
	Bassily and Dickinson [54]		124.223	98.926	93.770
	Present		124.0154	98.7626	93.5795
Edges length *b* simply supported, edges length a clamped	Cook and Rockey [55]		124.36	66.32	60.50
	Bassily and Dickinson [54]		124.223	66.336	58.615
	Present		124.0154	66.2213	58.5

Table 2
Comparison of the DQM results with those of the Galerkin method for nonlocal orthotropic plates.

$e_0 l_i \ (nm)$	Number of basic functions					DQM
	4	6	8	10	12	
0	19.2686	19.2686	19.2686	19.2686	19.2686	19.2686
0.5	18.7818	18.7818	18.7818	18.7818	18.7818	18.7818
1	17.4877	17.4876	17.4875	17.4875	17.4875	17.4875
1.5	15.7293	15.7291	15.7289	15.7289	15.7289	15.7289
2	13.7679	13.7675	13.7673	13.7673	13.7673	13.7673

In the absence of similar publications in the literature covering the same scope of the problem, one cannot directly validate the results found here. However, the present work could be partially validated based on a simplified analysis suggested by Bassily and Dickinson [54], Cook and Rockey [55] and Budiansky and Connor [49] on buckling of the local solution for which the nonlocal solution in this paper was ignored. In order to establish the accuracy and applicability of the proposed model, the numerical results are presented to compare with those available in the literature. The non-dimensional natural frequency becomes equal to zero when the shear in-plane loads achieve their critical value and the plate is likely to reach the flexural buckling state. The comparison of the critical shear load for isotropic plate and without considering the elastic medium is presented in Table 1. for different aspet ratios against results presented by Bassily and Dickinson [54], Cook and Rockey [55] and Budiansky and Connor [56]. It can be seen that the results herein exactly match with the other results reported.

In addition, the capability of the DQM in capturing the vibration frequency of the orthotropic nanoplates is investigated. To this end, the predicted results by the DQ technique are compared with those of the Galerkin method for the SSSS (simply supported along all edges) boundary condition. The numerical results (DQM and Galerkin method results) are listed in Table 2. Different number of basic function and various nonlocal parameters are considered. The dimensions of the plate are a= 10 nm and h =0.34 nm (i.e., aspect ratio is taken as $\beta = 1$). The shear in-plane load $\bar{P} = 10$ is considered in the computation. From Table 2. , one could observe that the present results by the DQ method are in good agreement with those of the Galerkin method solution. It should be noted that during calculations, it has been found that the total CPU time for the DQ technique is negligible compared to the CPU time

of the Galerkin method. Thus, DQ method is computationally low-cost tool in the vibration analysis of rectangular graphene sheets.

To study the effect of non-dimensional shear in-plane load on the non-dimensional frequency, in this paragraph, the non-dimensional frequency versus shear in-plane load of orthotropic rectangular nanoplate is shown in Fig. 5. The length of rectangular nanoplate is 10 nm and all edge of rectangular nanoplate is assumed clamped. The Fig. 5 depicts the fundamental natural frequency of vibration. The figures obviously indicate that the nonlocal effect has an important influence on the frequency vibration of a rectangular nanoplate under shear in-plane load. The decreasing rates of the natural frequencies become faster by increasing in the shear in-plane load. The non-dimensional natural frequency becomes equal to zero when the shear in-plane load attains their critical value; and the plate is likely to reach the flexural buckling state $(\Omega = 0)$. The intersection points of curves with the horizontal axis are the shear buckling loads of orthotropic rectangular nanoplate. The shear buckling loads continue to decrease when the nonlocal parameter becames larger. Therefore, the magnitudes of the shear in-plane loads are important parameter for the design of micro or nanoplate structures. These results are the same for other boundary conditions.

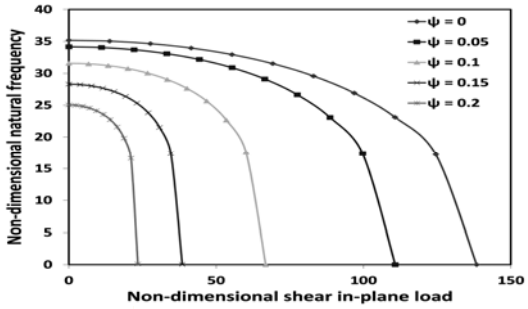

Fig. 5
Change of non-dimensional natural frequency with non-dimensional shear in-plane load for various nonlocal parameters and clamp boundary condition.

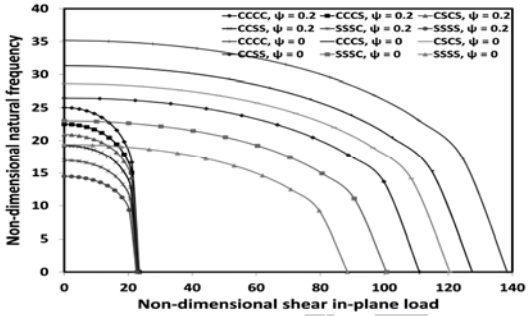

Fig. 6
Change of non-dimensional fundamental frequency of vibration with non-dimensional pre-load for various boundary condition with local and nonlocal models.

In Fig. 6 non-dimensional fundamental frequency calculated by local and nonlocal model is plotted versus non-dimensional shear in-plane loads for various boundary conditions. The first mode of vibration is considered and the length of orthotropic rectangular nanoplate is 10 nm. It is shown that the frequencies calculated by nonlocal model smaller than local model. Furthermore, the nonlocal effect also depends on the boundary conditions. The nonlocal effect kept on decreasing by became flexible the boundary conditions. The nonlocal effect for simply support boundary condition is much less than that for clamp boundary condition. The difference between any two boundary conditions decreases with increasing nonlocal parameter. The rectangular nanoplate with simply support boundary condition is earlier buckled because the rectangular nanoplate with clamp boundary conditions is more rigid than simply support boundary conditions. Consequently, the frequencies and the shear buckling loads for simply support boundary conditions are smaller than clamp boundary conditions.

To see the effect of small scale in different mode number the result from the solution for non-dimensional frequency rectangular nanoplate with different shear in-plane load $\overline{P} = 0,\ 10,\ 20$ are shown in Fig. 7. The variation for rectangular nanoplate with clamped boundary condition is plotted in Fig. 7. The length of nanoplate and aspect ratio are considered 10 nm and 1, respectively. It is found that the non-dimensional frequency increases with increase of mode number for all nonlocal parameters. Similar vibration response as that of first mode is observed in

this figure. Nonlocal solutions are smaller than the corresponding classical (local) solutions. However, nonlocal effects are highly prominent in vibration of rectangular nanoplate of higher wave modes. In addition, highest effect in non-dimensional frequency values for different nonlocal parameters are found at larger shear in-plane load. It is seen that effect of small length scale is higher for higher wave modes. This can be clearly seen from Fig. 7. This phenomenon is due to the effect of small wavelength at higher wave numbers. At smaller wavelengths interactions between atoms increases which leads to an increase in the nonlocal effects. This means that at larger shear in-plane load and larger mode number, small scale parameter is important. Further, with the increase of nonlocal parameter the difference between the curves increases.

In this section, to illustrate the effect of boundary condition on vibration response, we plot non-dimensional buckling load versus nonlocal parameter for two different lengths (5 nm, 20 nm) of isotropic and orthotropic square graphene sheet. The non-dimensional vibration frequency of first mode number is considered. According to Figs. 8(a),(b), results in the same consequence by decreasing the nanoplate's length, under other boundary conditions. This means that at smaller lengths and larger shear in-plane load, boundary condition of nanoplate is not important. This is shown that the difference between the vibration frequency calculated by isotropic and orthotropic for nanoplate with shear in-plane load is larger as compression nanoplate without shear in-plane load. This means that at larger shear in-plane load, material property of nanoplate is important. Also, it is observed that the non-dimensional vibration frequency increases with increasing length of nanoplates. Further, it is seen from this results that the difference between the vibration frequency calculated by isotropic and orthotropic for nanoplate with CCCC boundary condition is higher than that for SSSS case. Furthermore, the gap between vibration frequency curves of isotropic and orthotropic nanoplates follows the order CCCC>CCCS> SCSC > CCSS >SSSC>SSSS

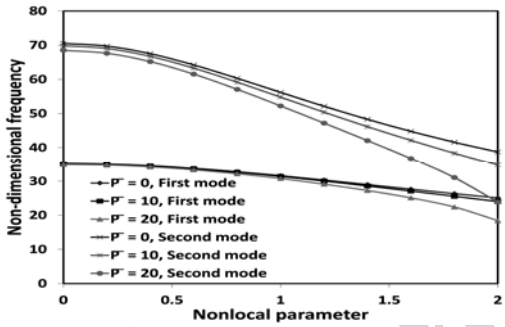

Fig. 7
Variation of non-dimensional frequency with nonlocal parameter for various shear in-plane load of rectangular nanoplate for first and second mode number.

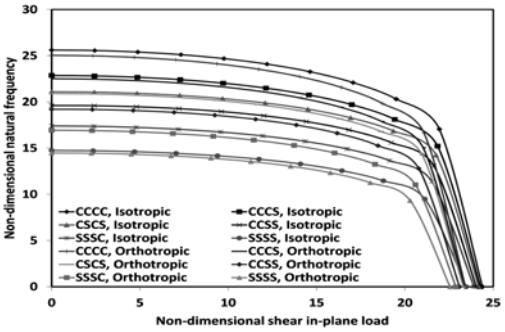

(a)

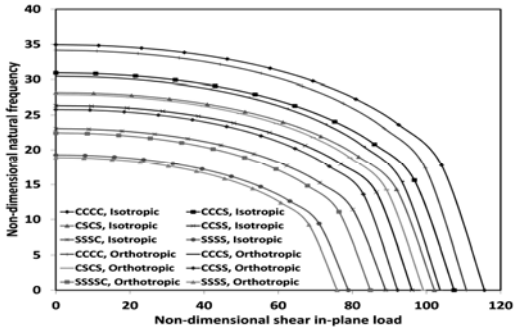

(b)

Fig.8
Effect of shear in-plane load on natural frequency of graphene sheet with isotropic and orthotropic property at various boundary conditions for (a) L= 5 nm and (b) L= 20nm.

In case of isotropic or orthotropic property, the difference between any two boundary conditions decreases with increasing shear in-plane load. In the present analyses of the six boundary conditions, maximum and minimum vibration frequencies are observed for CCCC and SSSS boundary conditions, respectively.

To see the effects of the surrounding elastic medium on rectangular graphene sheets, variation of fundamental frequencies with foundation parameters are plotted. Fig. 9 shows the effect of Winkler modulus parameter on the non-dimensional natural frequency of a rectangular graphene sheet with surrounding elastic medium modeled as Winkler foundation K_G=0. The effects of nonlocal parameters are also illustrated in the figure. The Winkler modulus parameter K_W, for the surrounding polymer matrix is taken in the range of 0–400. Similar values of modulus parameter were taken by Liew et al. [53] for the vibration analysis of double-layered graphene sheets DLGS embedded in polymer matrix. The vibration curves show that the fundamental frequencies are sensitive to the surrounding matrix. As the Winkler modulus parameter increases the fundamental frequencies also increase. This increasing trend of fundamental frequencies with surrounding matrix is noticed to be influenced significantly by small scale coefficients e_0l_i. For lower values of e_0l_i the vibration frequencies are higher while this is lower for large e_0l_i values. This interprets that if the rectangular graphene sheets are embedded in a soft elastic medium, vibration frequencies under shear in-plane load will be quite low for very small size rectangular graphene sheets as depicted in the figure.

Fig.10 shows the effect of shear modulus parameter on the fundamental frequencies of a rectangular graphene sheets with surrounding elastic matrix modeled as Pasternak foundation. A value of K_W=100 is taken in this elastic medium model. The shear modulus parameter K_G is varied from 0 to 10. These same values of modulus parameter were taken by Liew et al. [53] for the vibration analysis of double layer graphene sheets embedded in polymer matrix. As the value of shear modulus parameter increases, the vibration frequencies of rectangular graphene sheets increase. The vibration frequencies obtained from Pasternak foundation model are relatively larger than that obtained from the Winkler foundation model. Similar nonlocal effects are seen here. For higher e_0l_i value, the vibration frequencies with Pasternak foundation model are lower.

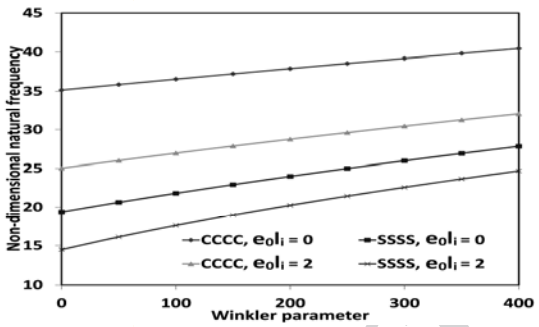

Fig. 9
Variation of non-dimensional frequency with Winkler elastic factor for two boundary conditions and nonlocal parameter.

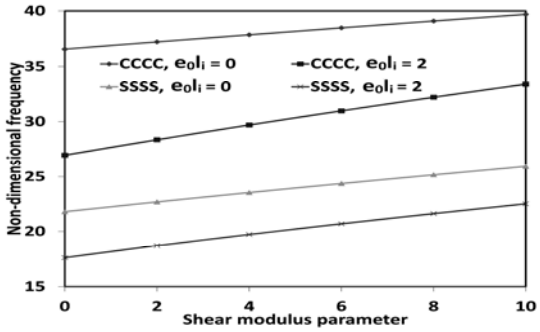

Fig. 10
Variation of non-dimensional frequency with shear modulus elastic factor for two boundary conditions and nonlocal parameter.

The relationships between frequency difference percent versus Winkler constant K_W and shear modulus K_G for different boundary condition and isotropic and orthotropic case are demonstrated in Figs. 11(a), (b). A scale coefficient e_0l_i = 1.0 nm is used in the analysis. The frequency difference percent is defined as:

$$\text{Difference percent}=\left|\frac{frequency_{\bar{P}\neq 0}-frequency_{\bar{P}=0}}{frequency_{\bar{P}=0}}\right|\times 100$$

As can be seen, the Winkler constant or shear modulus decreases then the effect of shear in-plane load on the difference percent increases. The shear in-plane load effect also depends on the boundary conditions as shown in Figs. 11(a), (b). As the boundary conditions became more flexible, the shear in-plane load effect kept on increasing. The shear in-plane load effect for SSSS boundary condition is much more than that for other boundary conditions.

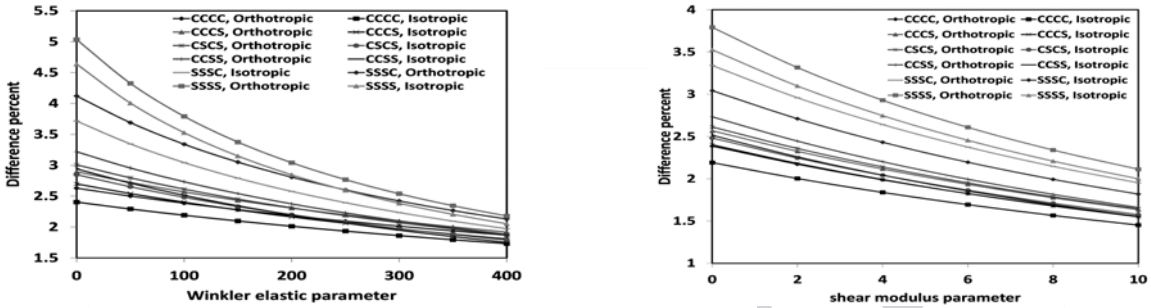

(a) (b)

Fig. 11
Variation of difference percent for various boundary conditions and isotropic and orthoropic property of graphene sheet for (a) Winkler elastic parameter and (b) Shear elastic parameter.

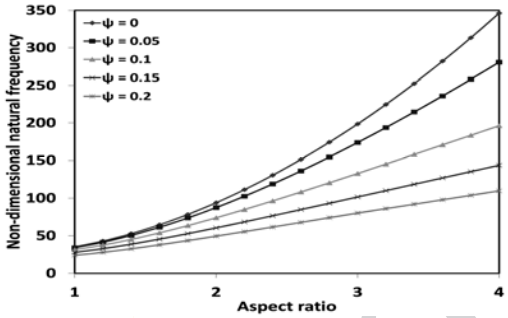

Fig. 12
Effect of aspect ratio on natural frequency for various nonlocal parameter.

Also, the difference percent for orthotropic case is larger than that for case of isotropic. From these plots obvious the important influence of boundary condition and shear in-plane load, in the cases isotropic and orthotropic case on the non-dimensional frequency of embedded graphene sheet.

Influence of nonlocal effects on the frequencies of nanoplate under shear in-plane load with various aspect ratios a /b is studied. Fig. 12 shows the variation in frequency with aspect ratio under various nonlocal parameters (e_0l_i /a). The nanoplate is assumed to be subjected to a normalized shear in-plane load of $\bar{P}=10$. It can be observed that as the aspect ratio increases, the non-dimensional frequency increases for all values of the nonlocal parameter. The results of figure indicate that, by increasing the values of nonlocal parameter, the non-dimensional frequency decreases for all values of aspect ratio. Also, it is observed that as the aspect ratio of the graphene sheet increases the effect of nonlocal parameter increases. Furthermore, as can be seen from Fig. 12, the non-dimensional frequency is sensitive to the small scale coefficient for large values of aspect ratio. In the other words, it is seen that the non-dimensional frequency for orthotropic small scale plates with higher aspect ratios (e.g., a/b = 4) are strongly affected by small scale than orthotropic small scale plates with lower aspect ratios (e.g., a/b = 2) and square ones.

We introduce a term 'frequency fraction' for the present study. Frequency fraction is defined as:

$$frequency\ \text{fraction}=\frac{\Omega_{Nonlocal}}{\Omega_{local}}$$

where $\Omega_{Nonlocal}$ and Ω_{Local} are the natural frequency which calculated using the nonlocal theory of elasticity $e_o l_i \neq 0$ and classical theory of elasticity $e_o l_i = 0$, respectively. The frequency fraction of the graphene sheet against the nonlocal parameter for various values of damper coefficient is plotted in Fig. 13. The damping modulus of damper $\bar{C}_d$ for the surrounding polymer matrix is gotten 50, 100, 150 and 200 respectively. The value of damping modulus damper was applied by Ghorbanpour Arani et al. [16, 18, 40 and 44]. As the values of the damper coefficient increase, the frequency ratio decreases. It is also observed that the effect of damper coefficient is not significant at lower nonlocal parameter while this effect is considerable at higher nonlocal parameter.

Frequency fraction of the sheet with respect to the nonlocal parameter for different medium of coupled system is demonstrated in Fig. 14. Four different cases of medium are considered. Case 1, Case2, Case 3 and Case 4 depict the (i) when the SLGS embedded by Winkler medium (ii) when the SLGS embedded by Pasternak medium (iii) when the SLGS embedded by Visco-Winkler medium (iv) when the SLGS embedded by Visco-Pasternak medium, respectively. Obviously, the effect of medium type on frequency ratio of the sheet becomes remarkable at higher nonlocal parameter. Also, the frequency ratio of Pasternak and Visco-Winkler mediums are maximum and minimum, respectively. Further, the medium effect on frequency ratio for coupled system follows the order

Pasternak medium > Visco-Pasternak medium > Winkler medium > Visco-Winkler medium

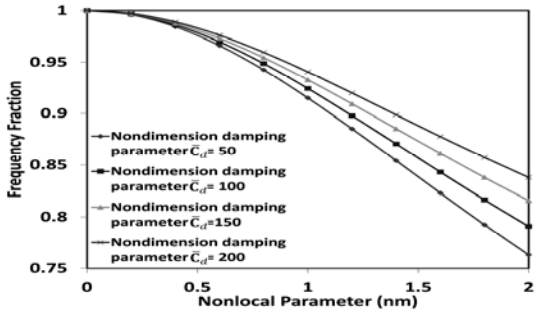

Fig. 13
Variation of frequency fraction with the nonlocal parameter for various damping modulus of damper.

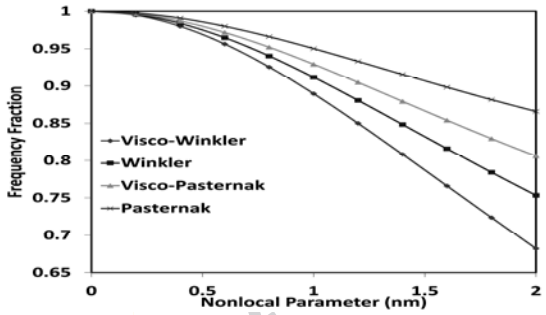

Fig. 14
Comparison frequency ratios of various medium of the graphene sheets.

The first few modes of vibration corresponding to the natural frequency are shown in Figs. 15(a),(b) and (c). In these figures are assumed simply supported boundary condition for all edge of rectangular nanoplate. The mode shape of orthotropic rectangular nanoplate plays a significant role in the design of the nanomechanical resonators. It is observed that the single-layered graphene sheet has a sinusoidal and cosine configuration.

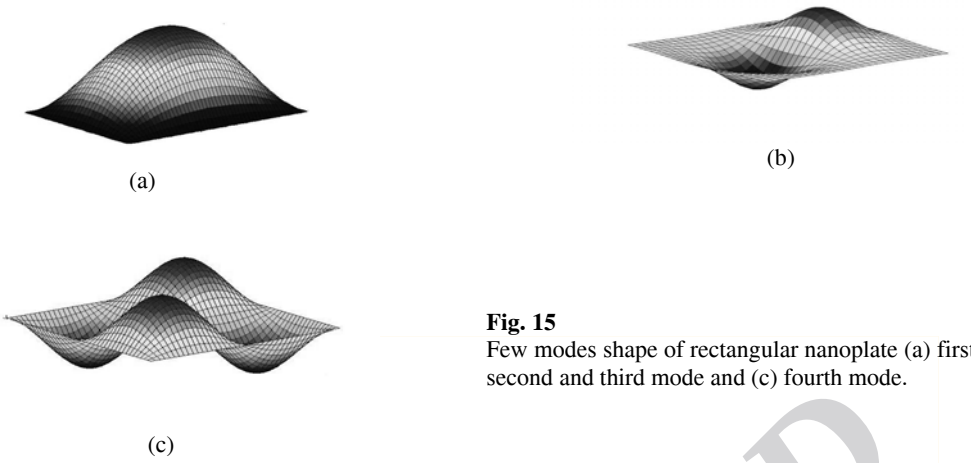

Fig. 15
Few modes shape of rectangular nanoplate (a) first mode, (b) second and third mode and (c) fourth mode.

The existence of the nonlocal parameter (e_0l_i) in the governing equation Eq. (13) takes into account the changes that are caused by the decrease in the size of a body at small scale. The influence of size on the behavior of nanomaterials is called size effect. Traditional elasticity theory cannot predict the size effects because it is independent of a scale factor (nonlocal parameter).The nonlocal parameter transforms the classical equations of local continuum mechanics into the corresponding governing equations of nonlocal continuum mechanics. This parameter (e_0l_i) is taken into the constitutive equations simply as a material constant. At small scale, size effects can be noticeable in the mechanical properties of nanostructures. Both molecular dynamics simulation and experimental studies have shown that the size effect plays a prominent role in the static and dynamic characteristics of nanostructures. As the dimensions of these structures are reduced, the effects of inter-molecular and inter-atomic interactions must be considered to predict mechanical behavior properly. The classical elasticity theory does not involve these effects. Thus, it is necessary to modify the classical theory to include small scale effects. In the nonlocal elasticity theory initiated by Eringen [22, 23], the small-scale effects are captured by assuming the stress at a point as a function not only of the strain at that point but also a function of the strains at all other points in the domain. The classical elasticity theory is a typical case of the nonlocal theory in which stress state at an arbitrary point depends only on the strain state at that point. The importance of the consideration of nonlocal scale coefficient is also explained in detail in the literature [22, 23, 26-30]. The nonlocal continuum theory based models contains information about the long-range forces between atoms and yields solution as a function of the size of structure. Chen et al. [57] investigated micro-continuum field theories such as couple stress theory, micromorphic theory, nonlocal theory, Cosserat theory, etc., from the atomistic viewpoint of lattice dynamics and molecular dynamics (MD) simulations. It is reported in their work that the nonlocal elasticity theory is physically reasonable. It should be noted that the classical local plate equation for the vibration of plate under shear in-plane load is obtained from Eq. (13) by making the nonlocal parameter equal to zero.

The internal characteristic length may be the lattice parameter or granular distance, but in the carbon nanostructures, it is often assumed to be the length of C–C bond (i.e., l_i= 0.142 nm) [29]. The choice of the value of parameter e_0 is vital for the validity of nonlocal models. This parameter is determined such that the nonlocal model calibrated with the experimental observations or the results of MD simulations. Eringen [22] equating the dispersive relation given by Born–Karman model of lattice dynamics to that of nonlocal theory for plane waves obtained a value of 0.39 for e_0. Wang and Hu [58] proposed an estimate of the value (e_0) around 0.288 using strain gradient method. Duan et al. [59] calibrated the value of nonlocal scaling parameter (e_0) for free vibration of single-walled carbon nanotubes using molecular dynamics simulations. They reported that the values of small scaling parameter vary between 0 to 19 depending on the length-to-diameter ratio, mode shape and boundary conditions of carbon nanotubes. Wang and Wang [60] presented the constitutive relations of nonlocal elasticity theory for application in the analysis of CNTs when modeled as Euler–Bernoulli beams, Timoshenko beams or as cylindrical shells. They also reported that the nonlocal parameter (e_0a) of CNTs must be smaller than 2.0 nm. Recently, these values for the

nonlocal parameter have been used by many researchers in stability and vibration problems at small scale [24-30]. Further, Shen et al. [61] estimated the nonlocal parameter (e_0l_i) for the nonlinear vibration analysis of SLGSs by matching the natural frequencies of graphene sheets observed from the MD simulation results with the numerical results obtained from the nonlocal plate model. In their paper, it is stated that the calibrated values of nonlocal parameter for the vibration analysis of rectangular armchair and zigzag monolayer graphene sheet (with length and width between 5-10 nm) at the room temperature (300 *K*) is in the range 0.27-0.67 nm and 0.22-0.47 nm, respectively.

6 CONCLUSIONS

Based on the nonlocal plate theory, the nonlocal effect on the vibration frequency of rectangular graphene sheets under shear in-plane load is investigated. Nonlocal elasticity theory has been applied to capture the structural discreteness of small-size plates (nanoplates). Equation of motion based on nonlocal theory has been derived. Numerical solutions are obtained for the non-dimensional frequency of nanoplates by employing the DQM. The validity of the present DQ technique is verified using the Galerkin method. Also, the presented approach is validated by performing the mechanical buckling analysis of isotropic rectangular plates and comparing the obtained solutions against existing results in other literatures. The effects of the nonlocal parameter on the vibration frequency of orthotropic and isotropic rectangular nanoplate embedded in an elastic medium was investigated for six cases boundary conditions. The elastic medium based on the Visco-Pasternak foundation was considered. It is found that the influence of the nonlocal parameter is quite significant in the vibration analysis of rectangular nanoplate and cannot be neglected. From the results of the present work, the following conclusions are noticeable:

- when the shear in-plane pre-loads attain their critical value the non-dimensional natural frequency becomes equal zero; and the plate is likely to reach the flexural buckling state.
- The decreasing rates of the natural frequencies become faster as the shear in-plane load increases.
- The small scale effects are more noticeable for the single-layered graphene sheets (SLGSs) with shear in-plane load compared to SLGSs without shear in-plane load.
- The effect of nonlocal parameter for higher mode number is important.
- The nonlocal effect depends on the boundary conditions. The nonlocal effect kept on decreasing by became flexible the boundary conditions.
- The difference between the vibration frequency calculated by isotropic and orthotropic for nanoplate with shear in-plane load is larger in compression with nanoplate without shear in-plane load.
- The difference between the vibration frequencies calculated by isotropic and orthotropic nanoplate for SSSS, SSSC, CCSS, SCSC, CCCS and CCCC boundary condition are in increasing order.
- The difference between any two boundary conditions decreases with increasing shear in-plane load.
- In the vibration analysis it is necessary to include the nonlocal elasticity theory for smaller orthotropic graphene sheets, smaller shear in-plane load and stiffer boundary conditions.
- The frequency values increases with an increase of Winkler and shear modulus factor.
- As the aspect ratio of the graphene sheet increases the effect of nonlocal parameter increases.
- The medium effect on frequency ratio for coupled system follows the order Pasternak medium > Visco-Pasternak medium > Winkler medium > Visco-Winkler medium

REFERENCES

[1] Li X., Bhushan B., Takashima K., Baek C.W., Kim Y.K., 2003, Mechanical characterization of micro/nanoscale structures for MEMS/NEMS applications using nano indentation techniques, *Ultramicroscopy* **97**:481-494.

[2] Fleck N. A., Muller G. M., Ashby M. F., Hutchinson J. W., 1994, Strain gradient plasticity: theory and experiment, *Acta Metallurgica et Materialia* **42**:475-487.

[3] Stolken J.S., Evans A.G., 1998, A microbend test method for measuring the plasticity length scale, *Acta Materialia* **46**: 5109-5115.

[4] Chong A.C.M, Yang F., Lam D.C.C, Tong P., 2001, Torsion and bending of micron-scaled structures, *Journal of Materials Research* **16**:1052-1058.

[5] Chowdhury R., Adhikari S., Wang C.W., Scarpa F., 2010, A molecular mechanics approach for the vibration of single walled carbon nanotubes, *Computational Material Science* **48**:730-735.

[6] Behfar K., Naghdabadi R., 2005, Nanoscale vibrational analysis of a multi-layered graphene sheet embedded in an elastic medium, *Composite Science Technology* **65**:1159-1164.

[7] Sakhaee-pour A., Ahmadian M.T., Naghdabadi R., 2008, Vibrational analysis of single-layered graphene sheets, *Nanotechnology* **19**(8):085702.

[8] Mohammadi M., Farajpour A., Goodarzi M., Dinari F., 2014, Thermo-mechanical vibration analysis of annular and circular graphene sheet embedded in an elastic medium, *Latin American Journal of Solids & Structures* **11**(4): 659-682.

[9] Mindlin R. D., Tiersten H. F., 1962, Effects of couple-stresses in linear elasticity, *Archive for Rational Mechanics and Analysis* **11**:415-448.

[10] Toupin R.A., 1962, Elastic materials with couple-stresses, *Archive for Rational Mechanics and Analysis* **11**:385-414.

[11] Akgöz B., Civalek Ö., 2013, Modeling and analysis of micro-sized plates resting on elastic medium using the modified couple stress theory, *Meccanica* **48**:863-873.

[12] Akgöz B., Civalek Ö., 2011, Strain gradiant and modified couple stress models for buckling analysis of axially loaded micro-scales beam, *International Journal of Engineering Science* **49**:1268-1280.

[13] Civalek Ö., Demir C., Akgöz B., 2010, Free vibration and bending analyses of cantilever microtubules based on nonlocal continuum model, *Mathematical and Computational Applications* **15**:289-298.

[14] Civalek Ö., Demir Ç., 2011, Bending analysis of microtubules using nonlocal Euler-Bernoulli beam theory, *Applied Mathematical Modeling* **35**:2053-2067.

[15] Farajpour A., Danesh M., Mohammadi M., 2011, Buckling analysis of variable thickness nanoplates using nonlocal continuum mechanics, *Physica E* **44**:719-727.

[16] Mohammadi M., Farajpour A., Goodarzi M., 2014, Numerical study of the effect of shear in-plane load on the vibration analysis of graphene sheet embedded in an elastic medium, *Computational Materials Science* **82**:510-520.

[17] Mohammadi M., Moradi A., Ghayour M., Farajpour A., 2014, Exact solution for thermo-mechanical vibration of orthotropic mono-layer graphene sheet embedded in an elastic medium, Latin *American Journal of Solids and Structures* **11**:437- 458.

[18] Ghorbanpour Arani A., Kolahchi R., Vossough H., 2012, Nonlocal wave propagation in an embedded DWBNNT conveying fluid via strain gradient, *Physica B: Condensed Matter* **407**:4281- 4286.

[19] Akgöz B., Civalek Ö., 2011, Application of strain gradient elasticity theory for buckling analysis of protein microtubules, *Current Applied Physics* **11**:1133-1138.

[20] Akgöz B., Civalek Ö., 2012, Analysis of micro-sized beams for various boundary conditions based on the strain gradient elasticity theory, *Archive of Applied Mechanics* **82**:423-443.

[21] Akgöz B., Civalek Ö., 2013, A size-dependent shear deformation beam model based on the strain gradient elasticity theory, *International Journal of Engineering Science* **70**:1-14.

[22] Eringen A.C., 1983, On differential equations of nonlocal elasticity and solutions of screw dislocation and surface waves, *Journal of Applied Physics* **54**:4703-4710.

[23] Eringen A. C., 2002, *Nonlocal Continuum Field Theories*, Springer, New York.

[24] Aydogdu M., 2009, Longitudinal wave propagation in nanorods using a general nonlocal unimodal rod theory and calibration of nonlocal parameter with lattice dynamics, *International Journal of Engineering Science* **56**:17-28.

[25] Aydogdu M., 2009, Axial vibration analysis of nanorods (carbon nanotubes) embedded in an elastic medium using nonlocal elasticity, *Mechanics Research Communications* **43**:34-40.

[26] Narendar S., Gopalakrishnan S., 2009, Nonlocal scale effects on wave propagation in multi-walled carbon nanotubes, *Computational Materials Science* **47**:526-538.

[27] Wang C. M., Duan W. H., 2008, Free vibration of nanorings/arches based on nonlocal elasticity, *Journal of Applied Physics* **104**:14303-14308.

[28] Moosavi H., Mohammadi M., Farajpour A., Shahidi S. H., 2011, Vibration analysis of nanorings using nonlocal continuum mechanics and shear deformable ring theory, *Physica E* **44**:135-140.

[29] Murmu T., Pradhan S. C., 2009, Buckling analysis of a single-walled carbon nanotube embedded in an elastic medium based on nonlocal elasticity and Timoshenko beam theory and using DQM, *Physica E* **41**:1232-1239.

[30] Wang Y. Z., Li F. M., Kishimoto K., 2011,Thermal effects on vibration properties of double layered nanoplates at small scales, *Composites Part B: Engineering* **42**:1311-1317.

[31] Reddy C.D., Rajendran S., Liew K. M., 2006, Equilibrium configuration and continuum elastic properties of finite sized graphene, *Nanotechnology* **17**:864-870.

[32] Malekzadeh P., Setoodeh A. R, Alibeygi Beni A., 2011, Small scale effect on the thermal buckling of orthotropic arbitrary straight-sided quadrilateral nanoplates embedded in an elastic medium, *Composite Structure* **93**: 2083-2089.

[33] Aksencer T., Aydogdu M., 2011, Levy type solution method for vibration and buckling of nanoplates using nonlocal elasticity theory, *Physica E* **43**:954-959.

[34] Satish N., Narendar S., Gopalakrishnan S., 2012, Thermal vibration analysis of orthotropic nanoplates based on nonlocal continuum mechanics, *Physica E* **44**:1950-1962.

[35] Prasanna T., Kumar J., Narendar S., Gopalakrishnan S., 2013, Thermal vibration analysis of monolayer graphene embedded in elastic medium based on nonlocal continuum mechanics, *Composite Structures* **100**: 332-342.

[36] Farajpour A., Mohammadi M., Shahidi A. R., Mahzoon M., 2011, Axisymmetric buckling of the circular graphene sheets with the nonlocal continuum plate model, *Physica E* **43**:1820-1825.

[37] Mohammadi M., Ghayour M., Farajpour A., 2013, Free transverse vibration analysis of circular and annular graphene sheets with various boundary conditions using the nonlocal continuum plate model, *Composites: Part B* **45**:32-42.

[38] Mohammadi M., Farajpour A., Moradi A., Ghayour M., 2014, Shear buckling of orthotropic rectangular graphene sheet embedded in an elastic medium in thermal environment, *Composites Part B* **56**:629-637.

[39] Farajpour A., Rastgoo A., Mohammadi M., 2014, Surface effects on the mechanical characteristics of microtubule networks in living cells, *Mechanics Research Communications* **57**:18-26.

[40] Ghorbanpour Arani A., Roudbari M.A., 2013, Nonlocal piezoelastic surface effect on the vibration of visco-Pasternak coupled boron nitride nanotube system under a moving nanoparticle, *Thin Solid Films* **542**:232-241.

[41] Farajpour A., Shahidi A. R., Mohammadi M., Mahzoon M., 2012, Buckling of orthotropic micro/nanoscale plates under linearly varying in-plane load via nonlocal continuum mechanics, *Composite Structures* **94**:1605-1615.

[42] Danesh M., Farajpour A., Mohammadi M., 2012, Axial vibration analysis of a tapered nanorod based on nonlocal elasticity theory and differential quadrature method, *Mechanics Research Communications* **39**:23-27.

[43] Mohammadi M., Ghayour M., Farajpour A., 2011, Analysis of free vibration sector plate based on elastic medium by using new version of differential quadrature method, *Journal of Solid Mechanics in Engineering* **3**:47-56.

[44] Mohammadi M., Goodarzi M., Ghayour M., Alivand S., 2012, Small scale effect on the vibration of orthotropic plates embedded in an elastic medium and under biaxial in-plane pre-load via nonlocal elasticity theory, *Journal of Solid Mechanics* **4**(2):128-143.

[45] Bert C. W, Malik M., 1996, Differential quadrature method in computational mechanics:a review, *Applied Mechanic Review* **49**:1-27.

[46] Shu C., Richards Be., 1992, Application of generalized differential quadrature to solve two-dimensional incompressible Navier Stokes equations, *International Journal for Numerical Methods in Fluids* **15**:791-798.

[47] Mohammadi M., Farajpour A., Goodarzi M., Mohammadi H., 2013, Temperature effect on vibration analysis of annular graphene sheet embedded on visco-pasternak foundation, *Journal of Solid Mechanics* **5**(3):305-323.

[48] Mohammadi M., Goodarzi M., Ghayour M., Alivand S., 2012, Small scale effect on the vibration of orthotropic plates embedded in an elastic medium and under biaxial in-plane pre-load via nonlocal elasticity theory, *Journal of Solid Mechanics* **4**:128-143.

[49] Mohammadi M., Goodarzi M., Farajpour A., Ghayour M., 2013, Influence of in-plane pre-load on the vibration frequency of circular graphene sheet via nonlocal continuum theory, *Composites: Part B* **51**:121-129.

[50] Romeo G., Frulla G., 1997, Post-buckling behaviour of graphite/epoxy stiffened panels with initial imperfections subjected to eccentric biaxial compression loading, *International Journal of Non-Linear Mechanics* **32**:1017-1033.

[51] Saadatpour M. M., Azhari M., 1998, The Galerkin method for static analysis of simply supported plates of general shape, *Computers and Structures* **69**:1-9.

[52] Babaei H., Shahidi A. R., 2011, Small-scale effects on the buckling of quadrilateral nanoplates based on nonlocal elasticity theory using the Galerkin method, *Archive of Applied Mechanics* **81**:1051-1062.

[53] Mohammadi M., Farajpour A., Goodarzi M., Heydarshenas R., 2013, Levy type solution for nonlocal thermo-mechanical vibration of orthotropic mono-layer graphene sheet embedded in an elastic medium, *Journal of Solid Mechanics* **5**(2):116-132.

[54] Bassilya S. F., Dickinson M., 1972, Buckling and lateral vibration of rectangular plates subject to in-plane loads a Ritz approach, *Journal of Sound and Vibration* **24**:219-239.

[55] Cook I.T., Rockey K.C., 1963, Shear buckling of rectangular plates with mixed boundary conditions, *Aeronautical Quarterly* **14**:349-356.

[56] Bijdiansky B., Connor R.W., 1948, *Buckling Stress of Clamped Rectangular Flat Plate in Shear*, Langley Memorial Aeronautical Laboratory, Langley Field, Virginia.

[57] Chen Y., Lee J.D., Eskandarian A., 2004, Atomistic viewpoint of the applicability of microcontinuum theories, *International Journal of Solids and Structures* **41**:2085-2097.

[58] Wang L. F., Hu H.Y., 2005, Flexural wave propagation in single-walled carbon nanotubes, *Physical Review B* **71**: 195412-195419.

[59] Duan W.H., Wang C. M., Zhang Y. Y., 2007, Calibration of nonlocal scaling effect parameter for free vibration of carbon nanotubes by molecular dynamics, *Journal of Applied Physics* **101**: 024305.

[60] Wang Q., Wang C. M., 2007, The constitutive relation and small scale parameter of nonlocal continuum mechanics for modelling carbon nanotubes, *Nanotechnology* **18**: 075702.

[61] Shen L., Shen S. H., Zhang C. L., 2010, Nonlocal plate model for nonlinear vibration of single layer graphene sheets in thermal environments, *Computational Materials Science* **48**:680-685.